

# Transport and Structural Study of the Pressure Induced Magnetic States in $\text{Nd}_{0.55}\text{Sr}_{0.45}\text{MnO}_3$ and $\text{Nd}_{0.5}\text{Sr}_{0.5}\text{MnO}_3$

Congwu Cui and Trevor A. Tyson

Physics Department, New Jersey Institute of Technology, Newark, New Jersey 07102

Zhong Zhong

National Synchrotron Light Source, Brookhaven National Laboratory, Upton, NY 11973

## ABSTRACT

Pressure effects on the electron transport and structure of  $\text{Nd}_{1-x}\text{Sr}_x\text{MnO}_3$  ( $x = 0.45, 0.5$ ) were investigated in the range from ambient to  $\sim 6$  GPa. In  $\text{Nd}_{0.55}\text{Sr}_{0.45}\text{MnO}_3$ , the low temperature ferromagnetic metallic state is suppressed and a low temperature insulating state is induced by pressure. In  $\text{Nd}_{0.5}\text{Sr}_{0.5}\text{MnO}_3$ , the CE-type antiferromagnetic charge ordering state is suppressed. Under pressure, both samples have a similar electron transport behavior although their ambient ground states are much different. It is surmised that pressure induces an A-type antiferromagnetic state at low temperature in both compounds.

PACS numbers: 62.50.+p, 71.27.+a, 75.25.+z, 75.47.Lx

## I. Introduction

In  $\text{Nd}_{1-x}\text{Sr}_x\text{MnO}_3$  manganite, the size difference between  $\text{Nd}^{3+}$  and  $\text{Sr}^{2+}$  is large ( $\sim 0.15$  Å). With increasing  $\text{Sr}^{2+}$  concentration, the bandwidth is increased. With changes in  $x$ , interesting spin, charge and orbital phases are produced and extensive studies have been performed.<sup>1</sup>

In the  $x = 0.5$  compound, on cooling from room temperature, there exist a transition from a paramagnetic insulating (PMI) phase to a ferromagnetic metallic (FMM) phase at  $\sim 255$  K and a transition from FMM phase to charge ordered (CO) antiferromagnetic (AF) insulating (AFI) phase at  $\sim 155$  K. The magnetic structure in CO AFI phase is CE-type.<sup>2</sup> With the application of a magnetic field, the FMM state is enhanced and the charge ordering state is suppressed completely above 7 T.<sup>3</sup> The magnetic field induced collapse of CO state is accompanied by a structural transition in which the volume increases drastically, leading to large positive magnetovolume effect.<sup>4</sup> Orbital ordering (OO) coincides with charge ordering. Different orbital ordering types,  $d_{3x^2-r^2}/d_{3y^2-r^2}$ -type<sup>5</sup> or  $d_{x^2-y^2}$ -type,<sup>6</sup> have been suggested in this compound.

$\text{Nd}_{0.45}\text{Sr}_{0.55}\text{Mn}_3$  is an A-type antiferromagnetic metal with coupled magnetic and structure transition at  $\sim 225$  K.<sup>2</sup> The Mn moments are ferromagnetically aligned in ab-plane in Pbnm symmetry. Charge carriers are confined within the ab-plane while the transport along c-axis is quenched, leading to highly anisotropic resistivity ( $\rho_c/\rho_{ab} \sim 10^4$  at 35 mK).<sup>7</sup> The antiferromagnetic spin ordering is accompanied by the  $d_{x^2-y^2}$ -type orbital ordering,

both of which are simultaneously destroyed by high magnetic fields, accompanied by a discontinuous decrease of resistivity.<sup>8</sup>

In this manganite system, the magnetic, electronic and orbital transitions are correlated to an abrupt structure transition, in which the a and b lattice constants are elongated and c is compressed (in Pbnm symmetry).<sup>7</sup> Other groups showed that in  $\text{Nd}_{0.5}\text{Sr}_{0.5}\text{MnO}_3$ , during the transition from FMM to AFI CO state, the crystal symmetry is lowered to monoclinic P21/m.<sup>9,10</sup> Ritter *et al.*<sup>11</sup> suggested that the low temperature AFI CO phase is phase-segregated into two different crystallographic structures and three magnetic phases: orthorhombic (Imma) ferromagnetic, orthorhombic (Imma) A-type antiferromagnetic, and monoclinic (P21/m) charge-ordered CE-type antiferromagnetic phases, in which a magnetic field can induce the charge-ordered monoclinic phase to collapse and to transform into the FMM orthorhombic phase. Kajimoto *et al.*<sup>12</sup> showed that in CE-type and A-type AF state, the  $\text{MnO}_6$  octahedra are apically compressed corresponding to  $d_{3x^2-r^2}/d_{3y^2-r^2}$  or  $d_{x^2-y^2}$  orbital ordering.

Hydrostatic and uniaxial pressure affect CO and FMM states differently. In  $\text{Nd}_{0.5}\text{Sr}_{0.5}\text{MnO}_3$ , hydrostatic pressure ( $<\sim 1$  GPa) increases  $T_C$  with  $dT_C/dP = 6.8$  K/GPa and decrease  $T_{CO}$  at a rate of 8.4 K/GPa,<sup>13</sup> while uniaxial pressure along the c-axis decreases  $T_C$  at a rate of 0.06 K/MPa and increases  $T_{CO}$  at a rate of 0.19 K/MPa.<sup>14</sup> In  $\text{Nd}_{0.45}\text{Sr}_{0.55}\text{MnO}_3$ , with the application of uniaxial pressure along the c-axis, the A-type antiferromagnetic phase is stabilized by increasing  $T_N$  at 0.066 K/MPa, implying the stabilization of the  $d_{x^2-y^2}$  orbital.<sup>14</sup> In thin films, due to the effect of substrate, biaxial

strain is induced. In  $\text{Nd}_{0.5}\text{Sr}_{0.5}\text{MnO}_3$  thin films, the thickness dependent strain tunes the competition between CO insulating and FMM state,<sup>15</sup> and there are optimal strains for which the CO or metallic states appear.<sup>16</sup>

The correlation between structure and electronic and magnetic transitions indicates its crucial role in this doping system. By applying high pressure up to  $\sim 6$  GPa, we studied the CO, FMM, AFM state changes in  $\text{Nd}_{0.55}\text{Sr}_{0.45}\text{MnO}_3$  and  $\text{Nd}_{0.5}\text{Sr}_{0.5}\text{MnO}_3$  through resistivity and structure measurements. It is found that pressure induces a similar electronic and magnetic behavior in them, which can be partly correlated to the orthorhombic distortion changes under pressure.

## II. Samples and Experimental Methods

The samples were prepared by solid-state reaction. Stoichiometric amounts of  $\text{Nd}_2\text{O}_3$ ,  $\text{MnO}_2$ , and  $\text{SrCO}_3$  powder were mixed, ground and calcined at  $900$   $^\circ\text{C}$  for 15 hours. The sample was then cooled down to room temperature and reground and then calcined again at  $1200$   $^\circ\text{C}$  for 17 hours. The powder was then pressed into pellets. The pellets were sintered at  $1500$   $^\circ\text{C}$  for 12 hours, cooled down to  $800$   $^\circ\text{C}$  at the rate  $5$   $^\circ\text{C}/\text{min}$ , then quickly cooled down to room temperature. The pellets were annealed at  $1200$   $^\circ\text{C}$  and cooled down slowly to room temperature at  $1$   $^\circ\text{C}/\text{min}$ . The x-ray diffraction patterns showed a single crystallographic phase for each sample. The magnetization and resistivity measurements are consistent with the results of other groups.<sup>1,17,18</sup> The details of the high-pressure resistivity and structural measurement methods were described elsewhere.<sup>19</sup>

### III. Results and Discussion

$\text{Nd}_{0.55}\text{Sr}_{0.45}\text{MnO}_3$  is a double exchange compound, with a FMM to PMI transition at  $\sim 280$  K upon warming. Under pressure, the electron transport is modified in an interesting manner. FIG. 1(a) is the resistivity as a function of temperature and pressure. The most important feature is the insulating state arising at low temperature under pressure. With pressure increase, the insulating behavior dominates above  $\sim 6$  GPa. Consequently, the resistivity in the measured temperature range changes with pressure [inset of FIG. 2(a)]. Below  $\sim 3.5$  GPa, the resistivity in the PMI phase is reduced while in FMM phase is almost unchanged. Above  $\sim 3.5$  GPa, in both phases, resistivity increases rapidly with pressure. In the low-pressure range, the metal-insulator transition temperature  $T_{\text{MI}}$  increases with pressure. Due to the limit of instrument (maximum temperature  $\sim 325$  K),  $T_{\text{MI}}$  above instrument upper limit in range of  $\sim 2\text{-}4$  GPa cannot be determined. Above  $\sim 4$  GPa, the transition temperature decreases on pressure increase. Above  $\sim 6$  GPa, the insulating behavior dominates so that the transition temperature can not be determined, although there is still a trace of metallic behavior. The transition temperature change under pressure is plotted in FIG. 2(a). The third-order polynomial fit gives a critical pressure  $P^* \sim 2.6$  GPa, while the resistivity in paramagnetic phase (at  $\sim 316$  K) gives  $P^* \sim 3.6$  GPa [inset of FIG. 2(a)].

In this compound, the behavior of  $T_{\text{MI}}$  and resistivity is similar to that found in manganites of  $\text{La}_{0.60}\text{Y}_{0.07}\text{Ca}_{0.33}\text{MnO}_3$ <sup>19</sup> and  $\text{Pr}_{0.7}\text{Ca}_{0.3}\text{MnO}_3$ .<sup>20</sup> However, the mechanism by which the material becomes insulating at high pressures is different. In those two

compounds, the material become insulating through the suppression of FMM state, displaying a decreasing  $T_{MI}$  above critical pressure. In  $Nd_{0.55}Sr_{0.45}MnO_3$ , the insulating state at high pressures has two origins: the suppression of FMM state and the expanding of a low temperature insulating phase, which appears with pressure increase and finally dominates at high pressures. The enhancement of the insulating phase is the dominant change in resistivity.

Abramovich *et al.*<sup>21</sup> proposed a phase-separation model in which the AFI droplets lie in a conducting FM host. In the phase-separation model, the behavior of the material becoming insulating can be understood as pressure induced percolation where the increasing pressure suppresses the FMM component and enhances AFI component above  $P^*$ .

It is noted that the transport behavior at high pressures where the compound becomes insulating is similar to that of  $Nd_{0.45}Sr_{0.55}MnO_3$  at ambient pressure.<sup>22</sup> When a high magnetic field of 35 T is applied, the resistivity of the A-type AF metallic  $Nd_{0.45}Sr_{0.55}MnO_3$  becomes similar to that of  $Nd_{0.55}Sr_{0.45}MnO_3$ , which is ascribed to the destruction of the A-type AF spin ordering and  $d_{x^2-y^2}$  orbital ordering.<sup>8</sup> Considering the similarity between the resistivity of  $x = 0.45$  compound under high pressure and  $x = 0.55$  at ambient pressure<sup>22</sup> and that of  $x = 0.55$  in high magnetic field,<sup>8</sup> one might speculate that the state induced by pressure in  $x = 0.45$  compound has a similar spin and orbital structure to  $Nd_{0.45}Sr_{0.55}MnO_3$ .

In FIG. 3(a), the compressibilities of lattice parameters (defined as  $\Delta a/a$ ,  $\Delta b/b$  and  $\Delta c/c$ ) are shown. The different compressibility leads to further distortion of the unit cell. To describe the orthorhombic distortion, Meneghini *et al.*<sup>23</sup> defined the ab-plane distortion ( $O_{ab} = 2 \frac{a-b}{a+b}$ ) and c-axis distortion ( $O_c = 2 \frac{a+b-c\sqrt{2}}{a+b+c\sqrt{2}}$ ) (in Pbnm symmetry). When the lattice is cubic, both  $O_{ab}$  and  $O_c$  are zero. FIG. 3(b) shows that both distortions increase under pressure, indicating a more distorted structure from the cubic case.

The structure of  $\text{Nd}_{0.45}\text{Sr}_{0.55}\text{MnO}_3$  is  $O^\dagger$  with  $a \approx b < \frac{c}{\sqrt{2}}$ . The corresponding orthorhombic distortion is  $\sim 0$  in ab-plane and -2% along c-axis (calculated with the data in ref. 12), which corresponds to the  $d_{x^2-y^2}$ -type orbital ordering and A-type AFM metal state. Under pressure, the orthorhombic distortion in both c-axis and ab-plane is increased in  $\text{Nd}_{0.55}\text{Sr}_{0.45}\text{MnO}_3$ , indicating that the high pressure structure is more different from  $\text{Nd}_{0.45}\text{Sr}_{0.55}\text{MnO}_3$  than at ambient pressure. The ab-plane distortion increase implies that the orbital state is different. However, the similarity between the resistivity (in both absolute value and shape) seems to suggest that pressure induces an A-type antiferromagnetic state in  $\text{Nd}_{0.55}\text{Sr}_{0.45}\text{MnO}_3$ .

FIG. 1(b) gives the resistivity of  $\text{Nd}_{0.5}\text{Sr}_{0.5}\text{MnO}_3$  under pressure. In the low temperature CO AFI phase, the resistivity is reduced by pressure. On the other hand, the insulating region extends to higher temperature so that the FM metallic state is suppressed. If the temperature where insulating and metallic state cross (the resistivity minimum) is defined as CO transition,  $T_{\text{CO}}$  increases with pressure and it seems to decrease above  $\sim 4$  GPa

[FIG. 2(b)]. In the mean time, pressure affects the metal-insulator transition only slightly. With pressure increase,  $T_{MI}$  increases below  $\sim 3$  GPa and drops above  $\sim 3$  GPa. The highest  $T_{MI}$  is only  $\sim 4$  K higher than at ambient pressure. In the measured pressure range, resistivity in the PMI phase is suppressed.

$T_{CO}$  increases with pressure below  $\sim 3.8$  GPa while  $T_{MI}$  shows almost no change [FIG. 2(b)]. This is different from that hydrostatic pressure ( $< 1$  GPa) increases  $T_C$  and decreases  $T_{CO}$  reported by other authors in single crystals.<sup>13</sup> On the contrary, our results are similar to the effects of uniaxial pressure along  $c$ -axis.<sup>14</sup> Under pressure, it was found that the  $c$ -axis distortion increases while the  $ab$ -plane distortion decreases with pressure [FIG. 3(c) and (d)]. Because the CO state corresponds to a higher orthorhombic distortion state,<sup>3</sup> possibly the pressure induced increase of  $c$ -axis distortion enhances the CO state. On the other hand, the slight  $ab$ -plane distortion decrease may enhance the electron hoping and lead to the resistivity decrease in the  $ab$ -plane.

Roy *et al.*<sup>24</sup> reported that pressure above  $\sim 1.5$  GPa can split the coincident antiferromagnetic and charge ordering transitions in which  $T_{CO}$  increases while  $T_N$  decreases. With the transitions decoupled, resistivity rises abruptly at the magnetic transition but not at CO transition, implying that low temperature resistivity comes mostly from the CE-type antiferromagnetic state. We did not observe the  $T_{CO}$  and  $T_N$  splitting in a larger pressure range, possibility because our sample is polycrystalline. However, the large suppression of resistivity indicates that the antiferromagnetic state,

specifically the CE-type AF state, is suppressed, which is also consistent to the ab-plane orthorhombic distortion reduction [FIG. 3(d)].

In  $\text{Nd}_{0.5}\text{Sr}_{0.5}\text{MnO}_3$ , by substituting  $\text{Nd}^{3+}$  with larger size  $\text{La}^{3+}$ , the bandwidth is increased and hence the CO phase is suppressed while  $T_C$  increases. With applied pressure, a transition from CO CE-type AFI to A-type AFI was suggested, in which resistivity is suppressed and  $T_{\text{CO}}$  gradually increases with pressure.<sup>25</sup> This is consistent with our result in the small bandwidth parent compound but at a much higher pressure. The smaller ab-plane distortion and larger c-axis distortion at high pressures may favor an A-type AF state and  $d_{x^2-y^2}$  orbital ordering as in the  $x = 0.55$  compound. In the A-type AFI state, resistivity is decreased due to enhanced in-plane transfer integral by the reduction of in-plane distortion. In the phase-separation model,<sup>11</sup> the A-type AF phase is enhanced and the CO CE-type AF phase is suppressed concomitantly by pressure. Because the bandwidth is sensitive to the local atomic structure of the  $\text{MnO}_6$  octahedra, especially the Mn-O-Mn bond angle, it is highly desired to measure the local atomic structure to explain the electronic and magnetic behavior under pressure.

The two  $\text{Nd}_{1-x}\text{Sr}_x\text{MnO}_3$  manganites at  $x = 0.45$  and 0.5 have very different electronic, magnetic and orbital ground states at ambient conditions. However, when we compare the resistivity at high pressure, we can find a surprising similarity between them [FIG. 1 (a) and (b)]. FIG. 4 is an example of the resistivity of these two compounds at pressures above the critical pressure. The similarity also seems to imply a similar electronic and magnetic state. The structural measurements partly justify this assumption. The

orthorhombic distortion of  $x = 0.45$  is increased by pressure to almost same as that of the  $x = 0.5$  compound at ambient pressure [FIG. 3(b) and (d)]. In addition, the similarity between the high pressure resistivity of these two compounds and that of  $\text{Nd}_{0.45}\text{Sr}_{0.55}\text{MnO}_3$  also suggests an A-type AFI phase in the high pressure phase.

It is interesting to compare the effects of pressure and strain in thin films. The inset of FIG. 4 is the resistivity of  $\text{Nd}_{0.5}\text{Sr}_{0.5}\text{MnO}_3$  thin films of several typical thickness from Prellier *et al.*<sup>15</sup> With thickness decrease, the strain in thin films is found to increase.<sup>16</sup> Compared with  $\text{Nd}_{0.55}\text{Sr}_{0.45}\text{MnO}_3$ , the resistivity evolution with thickness decrease (strain increase) is an analogy to pressure increase in bulk  $\text{Nd}_{0.55}\text{Sr}_{0.45}\text{MnO}_3$ , indicating that pressure increases strain in bulk sample proved by structure measurements.

#### IV. Summary

In summary, by studying the resistivity and structure of  $\text{Nd}_{1-x}\text{Sr}_x\text{MnO}_3$  ( $x = 0.45, 0.5$ ), it is found that they have a similar resistivity as a function of temperature, which results from the different effects of pressure on structure. Under pressure, both the ferromagnetic metallic state in the  $x = 0.45$  compound and the CE-type antiferromagnetic insulating state in the  $x = 0.5$  compound are suppressed. By comparing the resistivity and structure with the  $x = 0.55$  compound, pressure appears to induce a similar electronic and magnetic state in these two compounds with much different ground states. We suggest that the pressure induced magnetic states in both samples are A-type antiferromagnetic.

## **Acknowledgments**

The high pressure x-ray diffraction measurements were performed at beamline X17B1, NSLS, Brookhaven National Laboratory which is supported by US Department of Energy contract DE-AC02-76CH00016. The authors would like to thank Dr. Jingzhu Hu at X17C, NSLS for her help on the pressure calibration for x-ray diffraction. This work is supported by National Science Foundation Grant DMR-0209243.

## CAPTIONS

**FIG. 1 Resistivity of (a)  $\text{Nd}_{0.55}\text{Sr}_{0.45}\text{MnO}_3$  and (b)  $\text{Nd}_{0.5}\text{Sr}_{0.5}\text{MnO}_3$  under pressure.**

**FIG. 2 Transition temperatures of (a)  $\text{Nd}_{0.55}\text{Sr}_{0.45}\text{MnO}_3$  and (b)  $\text{Nd}_{0.5}\text{Sr}_{0.5}\text{MnO}_3$ .** The solid lines are third-order polynomial fits as guides to the eyes. (a) Metal-insulator transition temperature of  $\text{Nd}_{0.55}\text{Sr}_{0.45}\text{MnO}_3$  where the inset is the resistivity changes with pressure in PMI phase [at 316 K (solid circle) and FMM phase [at 120 K (open circle)]; (b) Metal-insulator transition (solid circle) and charge ordering transition (solid square) temperature of  $\text{Nd}_{0.5}\text{Sr}_{0.5}\text{MnO}_3$ .

**FIG. 3 Compressibility of lattice parameters and orthorhombic distortion of  $\text{Nd}_{0.55}\text{Sr}_{0.45}\text{MnO}_3$  and  $\text{Nd}_{0.5}\text{Sr}_{0.5}\text{MnO}_3$ .** Left panel: compressibility of lattice parameters (a) and the ab-plane and c-axis orthorhombic distortion (b) of  $\text{Nd}_{0.55}\text{Sr}_{0.45}\text{MnO}_3$ ; right panel: compressibility of lattice parameters (c) and ab-plane and c-axis orthorhombic distortion (d) of  $\text{Nd}_{0.5}\text{Sr}_{0.5}\text{MnO}_3$ . The solid lines in (a) and (c) are guides to the eye.

**FIG. 4 Comparison of resistivity of  $\text{Nd}_{0.55}\text{Sr}_{0.45}\text{MnO}_3$  and  $\text{Nd}_{0.5}\text{Sr}_{0.5}\text{MnO}_3$  under pressure.** The inset is the resistivity of  $\text{Nd}_{0.5}\text{Sr}_{0.5}\text{MnO}_3$  thin films with different thickness from Ref. 15 for comparison to our pressure results.

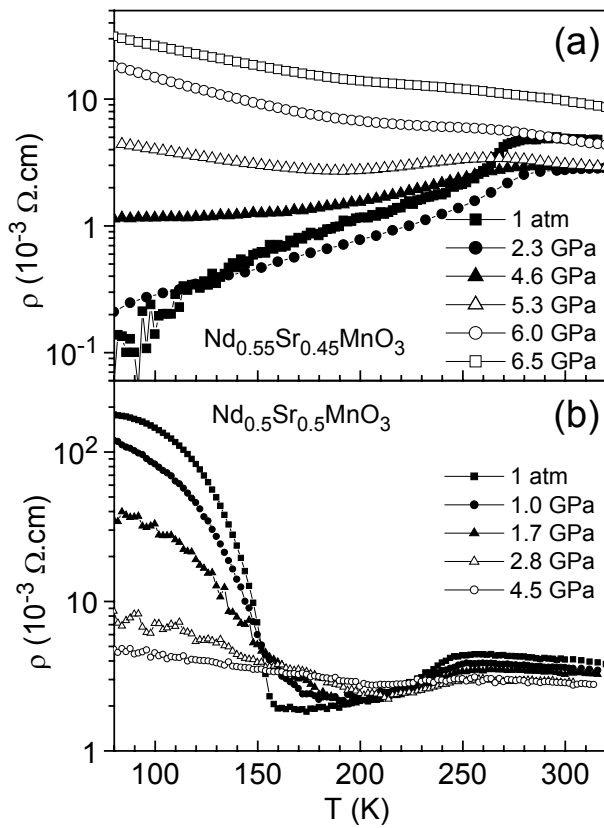


FIG. 1-CUI

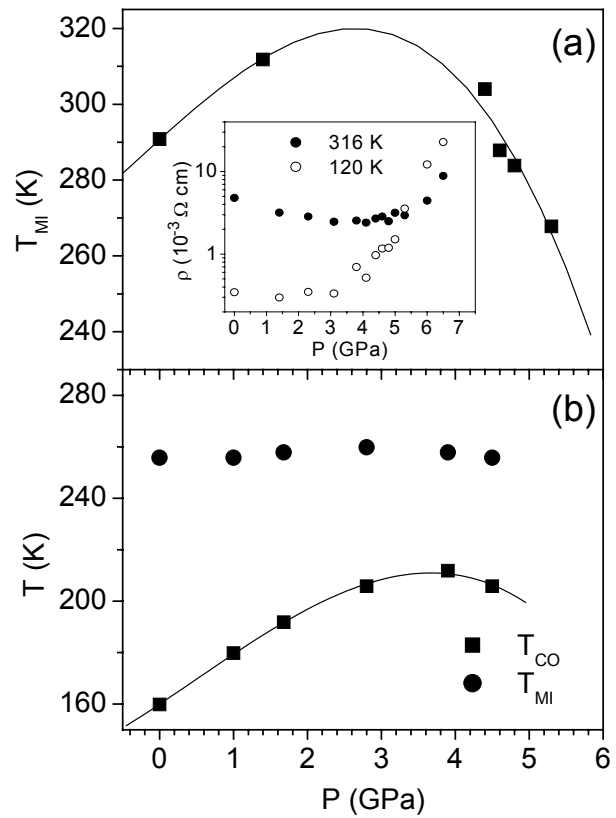


FIG. 2-CUI

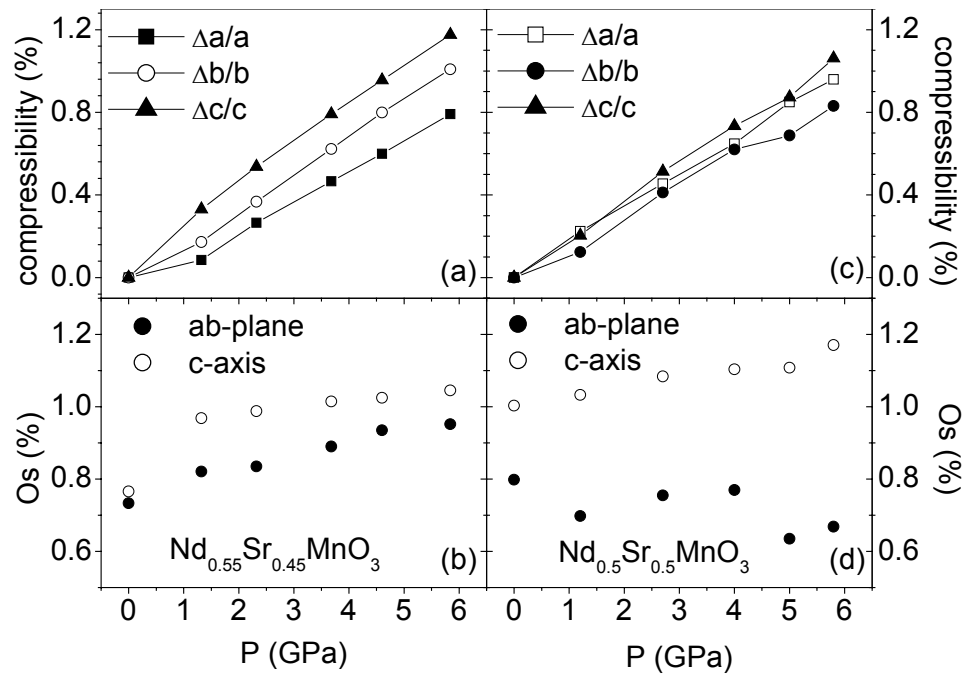


FIG. 3-CUI

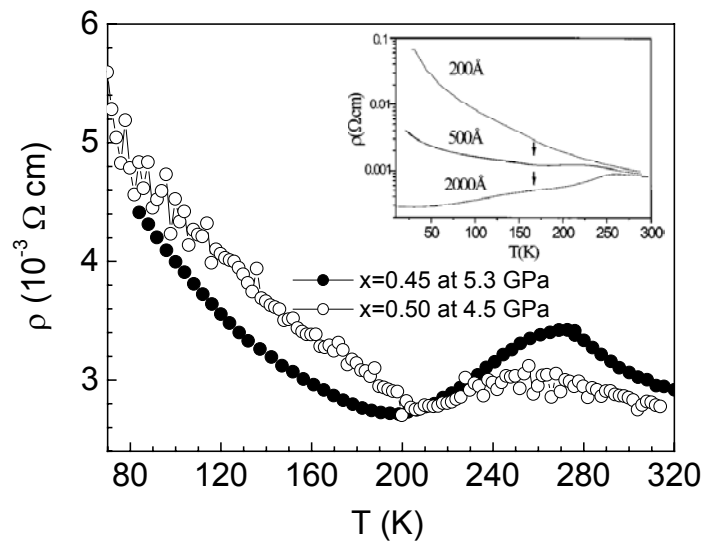


FIG. 4-CUI

## REFERENCES

<sup>1</sup> Y. Tokura and Y. Tomioka, *J. of Magn. and Magn. Mat.* **200**, 1 (1999).

<sup>2</sup> H. Kawano, R. Kajimoto, H. Yoshizawa, Y. Tomioka, H. Kuwahara, and Y. Tokura, *Phys. Rev. Lett.* **78**, 4253 (1997).

<sup>3</sup> H. Kuwahara, Y. Tomioka, A. Asamitsu, Y. Moritomo, and Y. Tokura, *Science* **270**, 961(1995).

<sup>4</sup> R. Mahendiran, M. R. Ibarra, A. Maignan, F. Millange, A. Arulraj, R. Mahesh, B. Raveau, and C. N. R. Rao, *Phys. Rev. Lett.* **82**, 2191 (1999).

<sup>5</sup> K. Nakamura, T. Arima, A. Nakazawa, Y. Wakabayashi, and Y. Murakami, *Phys. Rev. B* **60**, 2425 (1999).

<sup>6</sup> S. Zvyagin, A. Angerhofer, K. V. Kamenev L. -C. Brunel, G. Balakrishnan, and D. McK. Paul, *Solid State Commun.* **121**, 117 (2002).

<sup>7</sup> H. Kuwahara, T. Okuda, Y. Tomioka, T. Kimura, A. Asamitsu, and Y. Tokura, *Mat. Res. Soc. Symp. Proc.* 494, 83 (1998).

<sup>8</sup> T. Hayashi, N. Miura, K. Noda, H. Kuwahara, S. Okamoto, S. Ishihara, and S. Maekawa. *Phys. Rev. B* 65, 024408 (2002).

<sup>9</sup> V. Eremenko, S. Gnatchenko, N. Makedonska, Yu. Shabakayeva, M. Shvedun, V. Sirenko, J. Fink-Finowicki, K. V. Kamenev, G. Balakrishnan, and D. McK Paul, *Fizika Nizkikh Temperatur* 27, 1258 (2001).

<sup>10</sup> P. Laffez, G. Van Tendeloo, F. Millange, V. Caignaert, M. Hervieu, and B. Raveau, *Mater. Res. Bull.* 31, 905 (1996).

<sup>11</sup> C. Ritter, R. Mahendiran, M. R. Ibarra, L. Morellon, A. Maignan, B. Raveau, and C. N. R. Rao, Phys. Rev. B 61, R9229 (2000).

<sup>12</sup> R. Kajimoto, H. Yoshizawa, H. Kawano, H. Kuwahara, Y. Tokura, K. Ohoyama, and M. Ohashi, Phys. Rev. B **60**, 9506 (1999).

<sup>13</sup> Y. Moritomo, H. Kuwahara, and Y. Tokura, J. Phys. Soc. Jpn. **66**, 556 (1997).

<sup>14</sup> Taka-hisa Arima and Kenji Nakamura, Phys. Rev. B **60**, R15013 (1999).

<sup>15</sup> W. Prellier, A. Biswas, M. Rajeswari, T. Venkatesan, and R. L. Greene, Appl. Phys. Lett. **75**, 397 (1999).

<sup>16</sup> Q. Qian, T. A. Tyson, C.-C. Kao, W. Prellier, J. Bai, A. Biswas, and R. L. Greene, Phys. Rev. B **63**, 224424 (2001).

<sup>17</sup> V. Caignaert, F. Millange, M. Hervieu, E. Suard, and B. Raveau, Solid State Commun. **99**, 173 (1996).

<sup>18</sup> Y. Tomioka, H. Kuwahara, A. Asamitsu, M. Kasai, and Y. Tokura, Appl. Phys. Lett. **70**, 3609 (1997).

<sup>19</sup> Congwu Cui, Trevor A. Tyson, Zhong Zhong, Jeremy P. Carlo, and Yuhai Qin, Phys. Rev. B **67**, 104107 (2003).

<sup>20</sup> Congwu Cui and Trevor A. Tyson, unpublished.

<sup>21</sup> A. I. Abramovich, A. V. Michurin, O. Yu Gorbenko, and A. R. Kaul, J. Phys.: Condens. Matter **12**, L627 (2000).

<sup>22</sup> H. Kuwahara, T. Okuda, Y. Tomioka, A. Asamitsu, and Y. Tokura, Phys. Rev. Lett. **82**, 4316 (1999)

<sup>23</sup> C. Meneghini, D. Levy, S. Mobilio, M. Ortolani, M. Nuñez-Reguero, Ashwani Kumar, and D. D. Sarma, Phys. Rev. B **65**, 012111 (2001).

<sup>24</sup> A. S. Roy, A. Husmann, T. F. Rosenbaum, and J. F. Mitchell, Phys. Rev. B **63**, 094416 (2001)

<sup>25</sup> Y. Moritomo, H. Kuwahara, Y. Tomioka, and Y. Tokura, Phys. Rev. B **55**, 7549 (1997).